Available online at www.sciencedirect.com
SCIENCE DIRECT®
International Journal of Heat and Mass Transfer 47 (2004) 2961–2970
International Journal of HEAT and MASS TRANSFER
www.elsevier.com/locate/ijhmt

Constructal network for heat and mass transfer in a solid–gas reactive porous medium

Y. Azoumah *, N. Mazet, P. Neveu

IMP-CNRS UPR 8521, Institut de Science et Génie des Matériaux et Procédés, Tecnosud, Rambla de la Thermodynamique, 66100 Perpignan, France

Received 19 December 2003; received in revised form 11 March 2004

Abstract

The functioning of the solid–gas reactors is governed by several combined phenomena: heat and mass transfer and solid–gas chemical reaction. Heat and mass transfer phenomena have an antagonistic behavior in the reactive material used in the solid–gas reactors. This behavior of the material influences strongly both their power and energy performance and their design. In this paper, an optimal tree-shaped network for heat and mass transfer is constructed by using the constructal approach and the entropy generation minimisation method. The results of these optimisation show that, for a given heat and gas diffuser and a fixed porosity, we can find an optimal diffusers network design for any material. These optimal designs have the same minimum of entropy generation or "entropy generation number".

Keywords: Constructal theory; Entropy generation minimisation; Porous media; Solid–gas reactors

1. Introduction

Several emergent technologies involve solid–gas reactors, for example, energy conversion systems, natural gas storage and hydrogen storage [1,2], etc. The successful implementation of solid–gas reactors greatly depends on the transfer of heat and gas inside the porous active solid. This material then exhibits a strong coupling between heat and mass transfer and solid–gas chemical reaction. Two main ways can be used to improve the thermal characteristics of porous materials:

(i) Mixing the active solid with a highly conductive inert binder;
(ii) Compacting the active solid powder.

These two processes are combined in the manufacturing mode of reactive blocks developed by our laboratory, using expanded natural graphite (ENG) as binder [3].

These two processes may also lead to a decrease in mass flow. Fig. 1 shows the antagonistic evolution of the thermal conductivity and permeability of the active solid composite and the expanded natural graphite, versus the apparent density of this material in the composite [4,5]. There is a strong competition between the simultaneous improvement of heat and mass transfer in such active composites, and for this, one can vary the density of expanded natural graphite to manage the heat and mass transfer.

The performance of expanded natural graphite composites has a direct effect on the design of the reactor and on the whole thermochemical system. If the density of expanded natural graphite is low, heat exchangers must be added to increase heat transfer in the reactor. On the other hand, gas diffusers must be added to increase mass transfer in the reactor when the density of expanded natural graphite is high. The problem of gas diffusers distribution in a reactor was investigated by Jolly and Mazet [6] and Mazet et al. [7], where the number of the gas diffusers was fixed and the design

* Corresponding author. Fax: +33-468-682-213.
E-mail address: azoumah@univ-perp.fr (Y. Azoumah).

0017-9310/$ - see front matter © 2004 Elsevier Ltd. All rights reserved.
doi:10.1016/j.ijheatmasstransfer.2004.03.022

Nomenclature

A	affinity of reaction, J kg^{-1}
A_i	ith construct area, m^2
A_{ip}	heat and gas collector area for the ith construct, m^2
D_i	heat and gas collector thickness for ith construct, m
f_i	ith construct shape, $f_i = H_i/L_i$
h	gas specific enthalpy, J kg^{-1}
H_i	ith construct height, m
J_m	vapour mass flux density, kg m^{-2} s^{-1}
J_q	heat flux density, W m^{-2}
J_v	volume flux density, m s^{-1}
k_i	permeability of ith construct material, m^2
$\tilde{k}_i$	ratio of permeability, k_p/k_i
k_p	permeability of heat and gas collector, m^2
L_i	ith construct length, m
$\dot{m}$	volumetric rate of the gas, kg m^{-3} s^{-1}
$\dot{m}_i$	total gas flow rate for the ith construct, kg s^{-1}
n_i	number of $(i-1)$th constructs optimised in the ith construct
P	pressure, Pa
$P_i(\dot{\sigma})$	entropy generation rate of volume V_i, W K^{-1}
$\dot{q}$	volumetric heat generation rate, W m^{-3}
$\dot{q}_i$	total heat generation rate for the ith construct, W
r	heat of reaction, $r = \dot{q}/\dot{m}$, J kg^{-1}
S_i	entropy generation number of ith construct
T	temperature, K
V_i	ith construct volume, m^3
V_{ip}	heat and gas collector volume for ith construct, m^3
W	thickness of the material, m
$\dot{X}$	reaction rate, kg m^{-3} s^{-1}
x, y	Cartesian coordinates, m

Greek symbols

ε_i	ratio of dimensions, D_i/H_i
η	characteristic of the collector and the chemical system, $\eta = \lambda_p \mu T/k_p \rho^2 r^2$
ϕ_i	ratio of areas, A_{ip}/A_i
λ_i	thermal conductivity of ith construct material, W m^{-1} K^{-1}
λ_p	thermal conductivity of heat and gas collector, W m^{-1} K^{-1}
$\tilde{\lambda}_i$	ratio of thermal conductivity, λ_p/λ_i
μ	dynamic viscosity, kg m^{-1} s^{-1}
ν	kinematic viscosity, m^2 s^{-1}
ρ	gas density, kg m^{-3}
$\dot{\sigma}$	local entropy generation, W m^{-3} K^{-1}

Subscripts

i	construct of ith order
MT	mass transfer
min	minimum
max	maximum
opt	optimum
HT	heat transfer

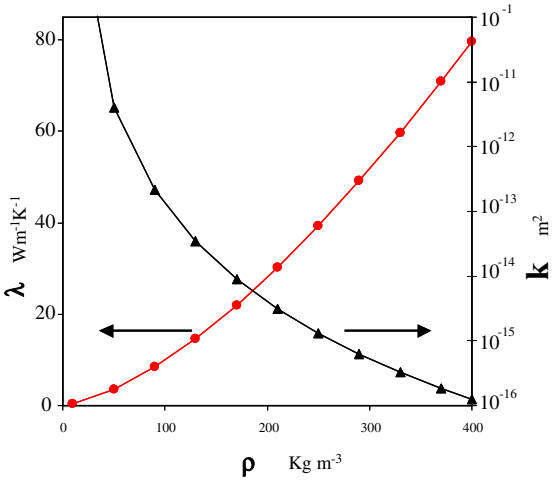

Fig. 1. The effect of density of the material on the permeability and thermal conductivity.

(configuration) of the reactor was also imposed. The objective of that work was to analyse the heat and mass transfer competition in active composite blocks.

The new problem considered in this paper is to find the optimal configuration: the number, size and position of gas diffusers and heat exchangers, for a given volume of an active material and a given exchanger area. This problem is quite close to the volume to point flow problem proposed by Bejan [8], on which contructal design was first proposed: for a given volume of reactor, what are the optimal number and size for both gas diffusers and heat exchangers? However, Bejan's criterion (minimisation of the maximum temperature difference [9], or pressure difference [10] within the system) cannot be used here, because of the coupling of the two driving forces, temperature and pressure gradients. The alternative we chose is the minimisation of the total entropy generation. This criterion was dictated by our domain of interest and its related objective: the improvement of exergy efficiency in energy conversion systems. It will be shown, however, that entropy generation minimisation

leads to Bejan's results when applied to a single transport phenomena.

In this paper, concepts of Thermodynamics of Irreversible Processes [11] are used in the description of the reactive material. This enabled us to quantify the total entropy generated by the system. Furthermore, Constructal design is performed in Section 3, and the results are later compared with Bejan's results. Finally, numerical examples, based on realistic materials, reveal some interesting constructal solid–gas reactor properties.

2. Solid–gas reactor model

This section reviews irreversible thermodynamics concepts in order to apply them to solid–gas systems. A solid–gas reactor contains a porous solid that is able to fix a certain amount of substance, which enters the reactor in vapour phase. Two types of thermodynamic systems can be used:

(i) Physical adsorption of a vapour on an adsorbent such as zeolite or active carbon;
(ii) Chemical reaction, consuming a solid S1 and producing a new compound S2, after reacting with the vapour. Chloride, nitrates, hydrates or hydrides can be used, depending on the nature of the vapour.

Although these two systems lead to different thermodynamics properties (e.g. pressure–temperature relationship), they are quite similar when transport phenomena are under consideration. For an adequate local description, both require a control volume that is at the same time sufficiently small so that pressure and temperature can be considered uniform, but sufficiently large to contain a large number of active sites. Both can be treated as a continuum, characterised by an equivalent thermal conductivity λ and equivalent permeability k_D. Finally, thermodynamic equilibrium is assumed at the local scale: adsorption or chemical kinetics are controlled by heat and mass transfer, and each active site imposes its equilibrium vapour pressure. As a consequence, the following derivations, which are carried out for chemical systems, are general and could be easily extended to adsorption systems.

2.1. Local entropy generation rate

The reactive porous medium with heat and mass flow is a mixture of expanded natural graphite and reactive solid (S1). This solid reacts with a gas (G) to produce a new solid (S2) according to the chemical reaction:

$$\mathrm{S1} + \mathrm{G} \rightarrow \mathrm{S2} \tag{1}$$

The reaction (1) generates heat that flows through the porous material from the active site to the heat exchanger while gas is consumed. The reaction (1) can also be performed in the reverse direction, by modifying the temperature-pressure constraint. In that case, solid (S1) and gas (G) are produced while heat is consumed and the flow of heat is from the collectors to the active sites.

Assuming that the Gibbs equation is valid at the local scale, mass conservation, energy conservation, and second law of thermodynamics lead to [12]:

$$\begin{aligned}
&\frac{\partial \rho}{\partial t} = -\nabla \cdot J_{\mathrm{m}} + \dot{m} \\
&\frac{\partial u}{\partial t} = -\nabla \cdot (J_q + J_{\mathrm{m}} h) \\
&\dot{\sigma} = J_q \cdot \nabla\left(\frac{1}{T}\right) + J_{\mathrm{v}} \cdot \left(\frac{\nabla P}{T}\right) + \frac{A}{T}\frac{\mathrm{d}X}{\mathrm{d}t}
\end{aligned} \tag{2}$$

Next, phenomenological laws are deduced from the local entropy generation expression, which displays the generalised forces related to each flux. By neglecting thermodynamic coupling, we obtain

$$\begin{aligned}
&J_q = L_q \nabla\left(\frac{1}{T}\right) \\
&J_{\mathrm{v}} = L_{\mathrm{v}} \frac{\nabla P}{T} \\
&\frac{\mathrm{d}X}{\mathrm{d}t} = L_X \frac{A}{T}
\end{aligned} \tag{3}$$

The phenomenological coefficients L_V and L_q can be deduced from the permeability and heat conductivity by comparing the phenomenological laws with the Darcy and Fourier laws. The coefficient L_X is in general assumed to be infinite. In this case the affinity must be equal to zero, in order to account for a finite chemical reaction rate. The infinite L_X is equivalent to the assumption that chemical equilibrium is maintained at the local scale. In summary, we obtain

$$L_q = \lambda T^2 \quad L_{\mathrm{v}} = \frac{k_{\mathrm{D}}}{\mu} T \quad L_X = \infty \tag{4}$$

When the local pressure and temperature remain constant in time, the system (2) becomes:

$$\dot{m} = -\rho \nabla \cdot J_{\mathrm{v}} \tag{5}$$

$$\dot{q} = -r\dot{m} = -\nabla \cdot J_q \tag{6}$$

$$\dot{\sigma} = J_q \cdot \nabla\left(\frac{1}{T}\right) + J_{\mathrm{v}} \cdot \left(\frac{\nabla P}{T}\right) + \frac{A}{T}\dot{m} \tag{7}$$

Eq. (3) shows that the mass and heat balances are coupled through the chemical reaction. In general, the integration of Eqs. (5)–(7) can be performed numerically by using the phenomenological laws (2) and the phenomenological coefficients (4). The entropy generation rate can then be evaluated.

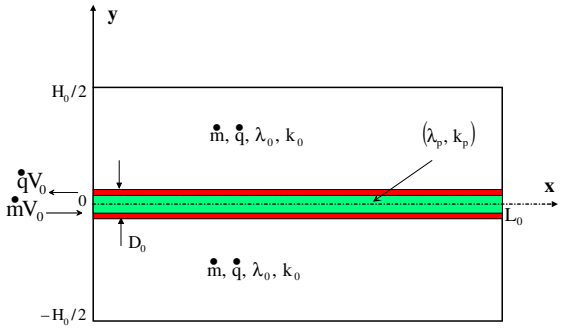

Fig. 2. Reactor model or elemental volume.

2.2. Solid–gas reactor

A parallelepiped elemental volume is chosen for this study; its cross-section area is represented in Fig. 2. This elemental volume is similar to the one that Bejan used to introduce the constructal method [11,12]. This permits the analytical integration of Eqs. (5)–(7), leading to a simple expression for entropy generation.

As shown in Fig. 2, the gas enters the elemental volume V_0 through a diffuser, for the chemical reaction, as described in the previous section. This reaction generates heat which is collected over the volume V_0 and lead to the heat sink, through heat collector, on its boundary (at $x = 0$; $-D_0/2 < y < D_0/2$).

It is important to note that heat collector and gas diffuser are combined in an element, which called "integrated heat and gas collector". This collector is characterised by a single length scale, the thickness D_0. This may seem difficult to realise in practice, however, this type of collector has already been studied [13].

3. Construction of the network of diffusers

The method of entropy generation minimisation or the minimisation of the dimensionless "entropy generation number" is used to optimise and to construct heat and gas collector network.

3.1. Elemental volume

Consider the elemental volume in Fig. 2, and assume that:

- The thermal conductivity and the permeability of the diffuser are much greater than the thermal conductivity and the permeability of the material. The dimensionless conductivity and permeability are defined as:

$$\tilde{\lambda}_0 = \frac{\lambda_p}{\lambda_0} \gg 1; \quad \tilde{k}_0 = \frac{k_p}{k_0} \gg 1 \tag{8}$$

- The walls of the system are adiabatic and impermeable except at the left end of the diffuser ($x = 0$; $-D_0/2 < y < D_0/2$) where a temperature T_0 and a pressure P_0 are imposed.
- The heat generation rate ($\dot{q}$) and the gas flow rate ($\dot{m}$) are uniformly distributed. The size of the elemental volume $A_0 = H_0 L_0$ is known and fixed, but the rectangular shape $f_0 = H_0/L_0$ may vary. The projected area of the collector is $A_{0p} = D_0 L_0$, where D_0 is its thickness. The heat and the gas flow geometry is two dimensional over the area A_0. Hence $V_0 = A_0 W$, where W is the dimension perpendicular to the plane of Fig. 2. According to the first assumption, the heat and gas flow vertically through the material, and horizontally through the diffuser. In addition, because of symmetry, we consider only one half of the system ($y \geqslant 0$).

The entropy generated inside the collector by heat conduction and gas flow is evaluated from Eqs. (5)–(7) by integrating in the x direction,

$$P_0(\dot{\sigma}_x) = 2\int_0^W \mathrm{d}z \int_0^{\frac{D_0}{2}} \mathrm{d}y \int_0^{L_0} \dot{\sigma}_x \,\mathrm{d}x \tag{9}$$

where

$$\dot{\sigma}_x = L_q \left[\frac{\partial}{\partial x}\left(\frac{1}{T}\right)\right]^2 + L_v \left[\frac{1}{T}\frac{\partial p}{\partial x}\right]^2$$

According to the Eq. (4) and the boundary conditions

$$x = L_0; \quad \frac{\partial T}{\partial x} = 0 \quad \text{and} \quad \frac{\partial P}{\partial x} = 0 \tag{10}$$

$$x = 0; \quad T(0) = T_0 \quad \text{and} \quad P(0) = P_0 \tag{11}$$

we obtain

$$P_0(\dot{\sigma}_x) = \frac{E_0}{3}\left[\frac{(1-\varepsilon_0)^2}{\varepsilon_0 f_0}\right] \tag{12}$$

where E_0 and ε_0 are

$$E_0 = \frac{(\dot{q}V_0)^2}{W\lambda_p T^2} + \frac{(\dot{m}V_0)^2\mu}{Wk_p T\rho^2} \quad \text{and} \quad \varepsilon_0 = D_0/H_0 \tag{13}$$

Note that ε_0 is the ratio between collector thickness and elemental volume height, and E_0 is a constant because $\dot{q}$, $\dot{m}$, the transfer properties of the collector (λ_p, k_p) and the thermodynamic properties of the solid–gas system (μ, ρ) are assumed constant.

Similarly, the entropy generated inside the elemental volume V_0 is obtained by integrating Eqs. (4)–(7) in the y direction subject to the boundary conditions:

$$y = \frac{H_0}{2}; \quad \frac{\partial T}{\partial y} = 0 \quad \text{and} \quad \frac{\partial P}{\partial y} = 0 \tag{14}$$

$$y = \frac{D_0}{2}; \quad T(0) = T_0 \quad \text{and} \quad P(0) = P_0 \tag{15}$$

We obtain

$$P_0(\dot{\sigma}_y) = \frac{(1-\varepsilon_0)^3 f_0}{12}\left(\frac{(\dot{q}V_0)^2}{W\lambda_0 T^2} + \frac{(\dot{m}V_0)^2\mu}{Wk_0T\rho^2}\right) \tag{16}$$

Notice that the latter factor differs from E_0 by the values of the thermal conductivity λ and the permeability k.

The total entropy generated inside the elemental volume is the sum

$$P_0(\dot{\sigma}) = P_0(\dot{\sigma}_x) + P_0(\dot{\sigma}_y)$$

which yields

$$P_0(\dot{\sigma}) = E_0\frac{(1-\varepsilon_0)^2}{3}\left[\frac{1}{\varepsilon_0 f_0} + \frac{1}{4}\left(\frac{\tilde{\lambda}_0 + \tilde{k}_0\eta}{1+\eta}\right)(1-\varepsilon_0)f_0\right] \tag{17}$$

Here η is a constant parameter depending on collector transfer properties and solid–gas thermodynamic properties

$$\eta = \frac{\lambda_p \mu T}{k_p \rho^2 r^2} \tag{18}$$

For conciseness in the presentation of general results, we use the dimensionless entropy generation number:

$$S_0(f_0) = \frac{P_0(\dot{\sigma})}{E_0} = \frac{(1-\varepsilon_0)^2}{3}\left[\frac{1}{\varepsilon_0 f_0} + \frac{1}{4}\left(\frac{\tilde{\lambda}_0 + \tilde{k}_0\eta}{1+\eta}\right)(1-\varepsilon_0)f_0\right] \tag{19}$$

For a given type of diffuser and reactive material, S_0 depends only on the shape f_0 and the the ratio between collector thickness and elemental volume height ε_0. When ε_0 is specified, the optimal shape can be determined by minimizing the entropy generation number:

$$\left(\frac{\partial S_0}{\partial f_0}\right)_{\varepsilon_0} = 0 \tag{20}$$

Results are reported in Table 1 for the single transfer ($\dot{m} = 0$, or $\dot{q} = 0$) and for coupled transfer ($\dot{q} = r\dot{m}$) and will be commented later.

3.2. Constructal sequence

3.2.1. First construct

Elemental volumes of fixed size and optimal shape are used to fill a large volume (V_1) as shown in Fig. 3. This first construct (A_1) contains n_1 elemental volumes, $A_1 = n_1 A_0$. The heat and the gas are carried by a new diffuser, which has the same thermal conductivity and permeability as the elemental diffuser (D_0) but its thickness is D_1.

Table 1
The optimal shape factors of the several constructs: comparison between the present results and those of Bejan [9,10]

		Shape factors	Unspecified value of ε_0	$\varepsilon_0 \ll 1$	Bejan [9,10] $\varepsilon_0 \ll 1$
Elemental volume	Heat transfer alone	$(f_0)_{S_{0HT}\text{opt}}$	$2(\varepsilon_0)^{-\frac{1}{2}}(\tilde{\lambda}_0)^{-\frac{1}{2}}(1-\varepsilon_0)^{-\frac{1}{2}}$	$2(\varepsilon_0)^{-\frac{1}{2}}(\tilde{\lambda}_0)^{-\frac{1}{2}}$	$2(\varepsilon_0)^{-\frac{1}{2}}(\tilde{\lambda}_0)^{-\frac{1}{2}}$
	Mass transfer alone	$(f_0)_{S_{0MT}\text{opt}}$	$2(\varepsilon_0)^{-\frac{1}{2}}(\tilde{k}_0)^{-\frac{1}{2}}(1-\varepsilon_0)^{-\frac{1}{2}}$	$2(\varepsilon_0)^{-\frac{1}{2}}(\tilde{k}_0)^{-\frac{1}{2}}$	$2(\varepsilon_0)^{-\frac{1}{2}}(\tilde{k}_0)^{-\frac{1}{2}}$
	Heat and mass transfer	$(f_0)_{S_0\text{opt}}$	$2(\varepsilon_0)^{-\frac{1}{2}}(1+\eta)^{-\frac{1}{2}}(\tilde{\lambda}_0 + \eta\tilde{k}_0)^{-\frac{1}{2}}(1-\varepsilon_0)^{-\frac{1}{2}}$	$2(\varepsilon_0)^{-\frac{1}{2}}(1+\eta)^{-\frac{1}{2}}(\tilde{\lambda}_0 + \eta\tilde{k}_0)^{-\frac{1}{2}}$	
Heat and mass transfer	First construct	$(f_1)_{S_1\text{opt}}$	$2(1-\phi_1)^{-\frac{1}{2}}(\varepsilon_{0\text{opt}})^{\frac{1}{2}}(\phi_1 - \varepsilon_{0\text{opt}})^{-\frac{1}{2}}(1-\varepsilon_{0\text{opt}})$ varies from 1.5 to 2	2	2
	Higher construct	$(f_i)_{S_i\text{opt}}\ i \geqslant 1$	$2(1-\phi_i)^{-\frac{1}{2}}(\varepsilon_{i-1\text{opt}})^{-\frac{1}{2}}(\phi_i - \varepsilon_{i-1\text{opt}})^{-\frac{1}{2}}(1-\varepsilon_{i-1\text{opt}})$		

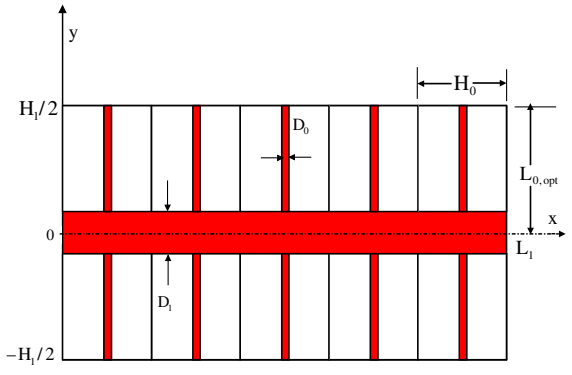

Fig. 3. First construct.

The first construct conducts heat and gas in almost the same way as the elemental volume. However, in the first construct the elemental material is replaced by a composite one. According to the assumption (8), the effective thermal conductivity and the effective permeability of the composite material are

$$\lambda_1 = \lambda_p \frac{D_0}{H_0} = \lambda_p \varepsilon_0 \quad \text{and} \quad k_1 = k_p \frac{D_0}{H_0} = k_p \varepsilon_0 \tag{21}$$

It is worth noting that the dimensionless conductivity and permeability are equal to $1/\varepsilon_0$:

$$\tilde{\lambda}_1 = \frac{\lambda_p}{\lambda_1} = \frac{1}{\varepsilon_0} \quad \text{and} \quad \tilde{k}_1 = \frac{k_p}{k_1} = \frac{1}{\varepsilon_0} \tag{22}$$

Similarly to the elemental volume, the expression of the entropy generated by the volume V_1 is

$$P_1(\dot{\sigma}) = E_1 \frac{(1-\varepsilon_1)^2}{3}\left[\frac{1}{\varepsilon_1 f_1} + \frac{1}{4\varepsilon_0}(1-\varepsilon_1) f_1\right] \tag{23}$$

where E_1, f_1 and ε_1 are respectively a constant parameter, the shape factor, and the dimensionless thickness of the first construct,

$$E_1 = (1+\eta)\frac{\dot{q}_1^2}{W \lambda_p T^2}, \quad f_1 = H_1/L_1, \quad \varepsilon_1 = D_1/H_1 \tag{24}$$

The total heat generated by the reactive mixture contained in the volume V_1 is $\dot{q}_1$. The entropy generation number of the first construct depends only on f_1, ε_1 and ε_0:

$$S_1(\varepsilon_0, \varepsilon_1, f_1) = \frac{P_1(\dot{\sigma})}{E_1} = \frac{(1-\varepsilon_1)^2}{3}\left[\frac{1}{\varepsilon_1 f_1} + \frac{1}{4\varepsilon_0}(1-\varepsilon_1) f_1\right] \tag{25}$$

In conclusion, we arrive at an optimisation problem with several variables. The Langrage multipliers method is used to solve this problem. The volume fraction of the collector allocated to A_1 is assumed fixed:

$$\phi_1 = \frac{A_{1p}}{A_1} = \varepsilon_1(1-\varepsilon_0) + \varepsilon_0 \tag{26}$$

The optimal shape, minimum entropy generation number, optimal number of elemental volumes, and optimal ratio of collector thicknesses are obtained by minimizing the aggregate expression:

$$\ell_1 = S_1 - \beta_1[\phi_1 - \varepsilon_1(1-\varepsilon_0) + \varepsilon_0] \tag{27}$$

with respect to f_1, ε_1 and ε_0, and by taking in account constraint (26).

In this expression β_1 is a Langrage multiplier. The results are presented in Tables 1 and 2.

3.2.2. Higher-order constructs

A larger volume (second construct) is designed next; by optimising the assembly of a number of first constructs. It is found that the expression for the entropy generation rate of ith construct is similar to that of the first construct. The general form of entropy generation number is

$$S_i(\varepsilon_{i-1}, \varepsilon_i, f_i) = \frac{P_i(\dot{\sigma})}{E_i} = \frac{(1-\varepsilon_i)^2}{3}\left[\frac{1}{\varepsilon_i f_i} + \frac{1}{4\varepsilon_{i-1}}(1-\varepsilon_i) f_i\right] \tag{28}$$

Table 2
The minimum entropy generation number, number of optimised constructs and ratio of collector thicknesses

$(S_0)_{\min}$	$\frac{1}{3}(\varepsilon_0)^{\frac{-1}{2}}(1-\varepsilon_0)^{\frac{5}{2}}(1+\eta)^{\frac{-1}{2}}(\tilde{\lambda}_0 + \eta\tilde{k}_0)^{\frac{1}{2}}$
$(S_1)_{\min}$	$\frac{1}{3}(1-\phi_1)^{\frac{5}{2}}(\varepsilon_{0\text{opt}})^{\frac{-1}{2}}(1-\varepsilon_{0\text{opt}})^{-2}(\phi_1 - \varepsilon_{0\text{opt}})^{\frac{-1}{2}}$
$(S_i)_{\min}\ i \geqslant 1$	$\frac{1}{3}(1-\phi_i)^{\frac{5}{2}}(\varepsilon_{i-1\text{opt}})^{\frac{-1}{2}}(1-\varepsilon_{i-1\text{opt}})^{-2}(\phi_i - \varepsilon_{i-1\text{opt}})^{\frac{-1}{2}}$
$n_{1\text{opt}}$	$(1-\phi_1)^{\frac{1}{2}}(\varepsilon_{0\text{opt}})^{\frac{-1}{2}}(1-\varepsilon_{0\text{opt}})^{\frac{-1}{2}}(\phi_1 - \varepsilon_{0\text{opt}})^{\frac{1}{2}}(1+\eta)^{\frac{-1}{2}}(\tilde{\lambda}_0 + \eta\tilde{k}_0)^{\frac{1}{2}}$
$n_{i\text{opt}}\ i \geqslant 2$	$(1-\phi_i)^{\frac{1}{2}}(\varepsilon_{i-1\text{opt}})^{\frac{-1}{2}}(1-\varepsilon_{i-1\text{opt}})^{-1}(\phi_i - \varepsilon_{i-1\text{opt}})^{\frac{1}{2}}(1+5\varepsilon_{i-1\text{opt}})^{\frac{1}{2}}(1+4\varepsilon_{i-1\text{opt}})^{\frac{-1}{2}}[-4(\varepsilon_{i-1\text{opt}})^2 + 3\varepsilon_{i-1\text{opt}} + 1]$
$(\frac{D_1}{D_0})_{\text{opt}}$	$(\varepsilon_{0\text{opt}})^{\frac{-1}{2}}(1-\varepsilon_{0\text{opt}})^{\frac{-1}{2}}(1+\eta)^{\frac{-1}{2}}(\tilde{\lambda}_0 + \eta\tilde{k}_0)^{\frac{1}{2}}(\phi_1 - \varepsilon_{0\text{opt}})$
$(\frac{D_i}{D_{i-1}})_{\text{opt}}\ i \geqslant 2$	$(\varepsilon_{i-1\text{opt}})^{-1}(1-\varepsilon_{i-1\text{opt}})^{-1}(1+5\varepsilon_{i-1\text{opt}})^{\frac{1}{2}}(1+4\varepsilon_{i-1\text{opt}})^{\frac{-1}{2}}(\phi_i - \varepsilon_{i-1\text{opt}})[-4(\varepsilon_{i-1\text{opt}})^2 + 3\varepsilon_{i-1\text{opt}} + 1]$

where

$$E_i = (1+\eta)\frac{\dot{q}_i^2}{W\lambda_p T^2} \quad f_i = H_i/L_i \quad \varepsilon_i = D_i/H_i \tag{29}$$

For a given heat power $\dot{q}_i$, total volume V_i, and collector volume fraction ϕ_i, the minimum total entropy generation can be found subject to the constraint:

$$\phi_i = \frac{A_{ip}}{A_i} = \varepsilon_i(1-\varepsilon_{i-1}) + \varepsilon_{i-1} \tag{30}$$

The method of Langrage multipliers delivers the optimal shape, minimum entropy generation number, optimal number of previous constructs, and optimal ratio of collector thicknesses. This is done by minimizing the function

$$\ell_i = S_i - \beta_i[\phi_i - \varepsilon_i(1-\varepsilon_{i-1}) + \varepsilon_{i-1}] \tag{31}$$

with respect to ε_{i-1}, ε_i and f_i, where β_i is a Langrage multiplier; and by using the constraint ϕ_i.

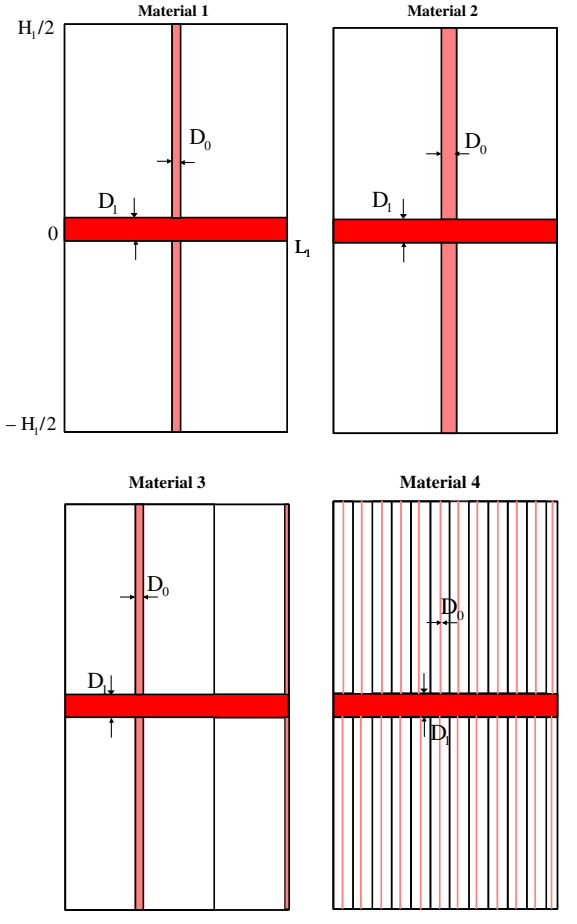

Fig. 4. Optimal designs for four different materials (Table 3).

4. Results and discussion

The results are reported in Tables 1 and 2, where

$$\varepsilon_{0\text{opt}} = \frac{1}{12}\left(5\phi_1 + 2 - (25\phi_1^2 - 4\phi_1 + 4)^{\frac{1}{2}}\right) \tag{32}$$

$$\varepsilon_{i-1\text{opt}} = \frac{1}{12}\left(5\phi_i + 2 - (25\phi_i^2 - 4\phi_i + 4)^{\frac{1}{2}}\right). \tag{33}$$

In Table 1 we see the optimal shapes obtained after the minimisation of the entropy generation number of several constructs. Later, a comparison is made with Bejan's results. The optimal shape of the elemental volume $(f_0)_{S_0\text{opt}}$ strongly depends on the medium porosity, the characteristics of the material and the collector, and the chemical system. On the other hand, from the first construct to higher-order constructs, the optimal shapes $(f_i)_{S_i\text{opt}}$ $(i \geqslant 1)$ depend only on the medium porosity.

Table 1 reveals several additional and important features. If $\varepsilon_0 \ll 1$, the optimal shapes obtained by entropy number minimisation of a single transfer, such as mass or heat transfer $[(f_0)_{S_{0\text{HT}}\text{opt}}, (f_0)_{S_{0\text{MT}}\text{opt}}]$ are the same as those obtained by the minimisation of driving forces. These optimal shapes are close to Bejan's results [9,10]. However, if we assume an unspecified value of ε_0, the additional factor $(1-\varepsilon_0)^{-1/2}$ appears in the expression of the optimal shape for a single transfer. We didn't make any assumption on ε_0 in order to allow the application of this study to a large range of solid–gas reactor configurations.

Table 1 also shows that the same additional factor $(1-\varepsilon_0)^{-1/2}$ appears in the expression of the optimal shape obtained by the optimisation of coupled mass and heat transfer when the value of ε_0 is not specified. This factor disappears from the expression of the same optimal shape when $\varepsilon_0 \ll 1$.

In Table 1 we also see that the optimal shape f_1 from the optimisation of the coupled transfer with $\varepsilon_0 \ll 1$ is constant and equal to 2. This is same as the results of Bejan [9]. On the other hand, when ε_0 is not specified, the optimal shape is not exactly equal to 2. This value varies from 1.5 to 2, as shown in Fig. 5.

The minimum entropy generation number of the elemental volume $(S_0)_{\min}$ depends on the medium porosity, the characteristics of the material and the collector, and the chemical system (see Table 2). Starting with the first construct, the minimum entropy generation number depends only on the medium porosity. This leads to an important design conclusion: an optimal design of solid–gas reactor can be found for any material. For a given collector, and for fixed porosity and area of the system, these optimal designs have the same minimum entropy generation number.

Table 2 also shows that the optimal number of elemental volumes in the first construct $n_{1\text{opt}}$ depends on the medium porosity, the characteristics of the material

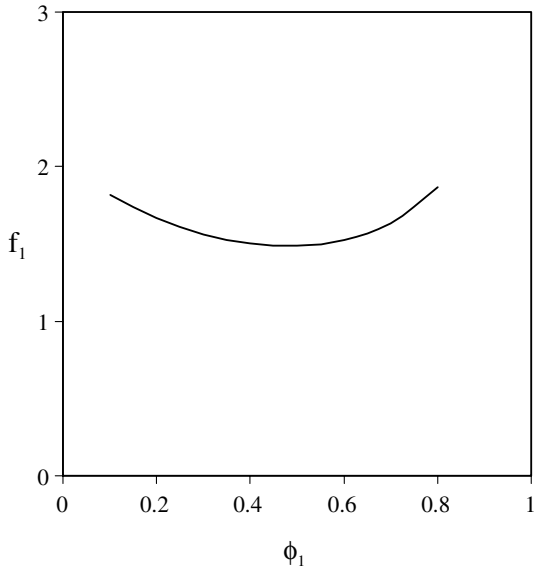

Fig. 5. The optimal shape of the first construct.

and the collector, and the chemical system. This remark also applies for the optimal ratio of collectors thickness $(D_1/D_0)_{\text{opt}}$. However, starting with the second construct, the optimal number of previously optimised constructs ($n_{i\text{opt}}$) and the optimal ratio of collector thicknesses $(D_i/D_{i-1})_{\text{opt}}$ depend only on the medium porosity.

5. Numerical example

Consider four different materials (Table 3) and an integrated heat and mass collector with specified properties: $k_p = 10^{-10}$ m^2 and $\lambda_p = 237$ W m^{-1} K^{-1}. In this section we compare the optimal network of heat and gas collectors for the four different materials. From the first to the fourth material, we have different density of expanded natural graphite: the first material is less dense than the second one, etc.

Table 3 shows the results of the optimisation at the first construct level, and the Fig. 4 presents the optimal network of diffusers corresponding to each material. Each material has an optimal network design. These optimal designs differ greatly from one material to another, and some of them are very complex from practical point of view. It is important to note that all these optimal designs have the same minimum entropy generation number. The practical conclusion is that we must choose the material that leads to the easiest design.

6. The competition between heat and mass transfer, or the distribution of entropy generation

Assume a material that have fixed characteristics $(\lambda_0, k_0, \mu, \rho, r)$, and a collector that has variable characteristics (λ_p, k_p). Fig. 6 shows the evolution of the entropy generation number accounting for heat and mass transfer in an elemental volume with $\phi_1 = 0.1$. Recall that $\eta = \lambda_p \mu T / k_p \rho^2 r^2$ characterises the collector and the chemical system. In fact, increasing η means increasing thermal conductivity relative to the permeability of the collector. The minimum entropy generation number for mass transfer increases when η increases while the min-

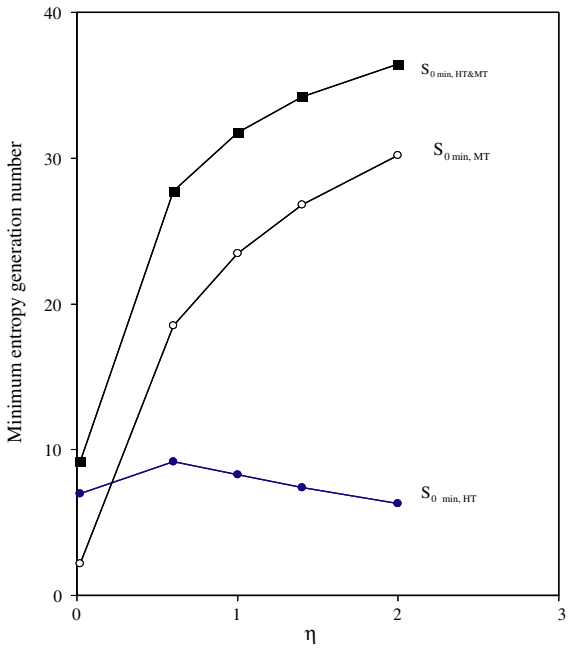

Fig. 6. The competition between heat and mass transfer at elemental-volume level.

Table 3
Four numerical examples of optimised structures when the transport properties of the materials are specified

	λ_0 (W m^{-1} K^{-1})	$\tilde{\lambda}_0$	k_0 (m^2)	$\tilde{k}_0$	ϕ_1	$\varepsilon_{0\text{opt}}$	$(f_1)_{S1\text{opt}}$	$(S_1)_{\min}$	$n_{1\text{opt}}$	$(\frac{D_1}{D_0})_{\text{opt}}$
Material 1	3	79	10^{-12}	10^2	0.1	0.0448	1.81	5.7	2	2.37
Material 2	10	23.7	10^{-13}	10^3	0.1	0.0448	1.81	5.7	1.36–2	1.59
Material 3	15	15.8	10^{-14}	10^4	0.1	0.0448	1.81	5.7	2.69–3	3.14
Material 4	30	7.9	10^{-16}	10^6	0.1	0.0448	1.81	5.7	25.3–26	29.65

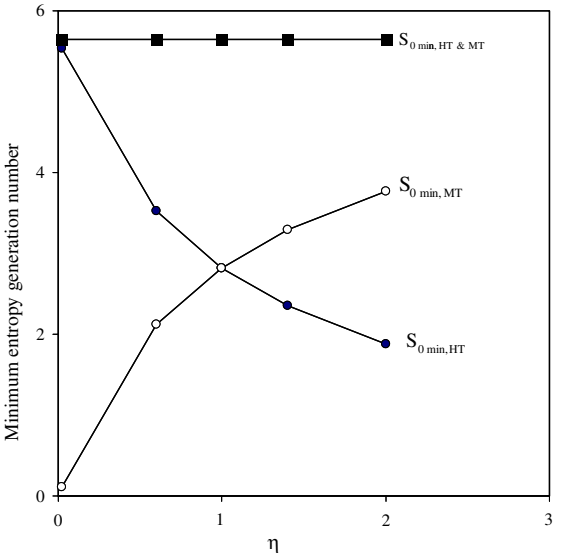

Fig. 7. The competition between heat and mass transfer at first-construct level.

imum entropy generation number for heat transfer decreases slightly. The total minimum entropy generation number also increases when η increases. We conclude that mass transfer is impeded when η becomes progressively larger; and at the limit case $\eta = 0$ the main limitation is the thermal conduction.

Fig. 7 shows the minimum entropy generation number for the first construct. We see the same behavior at the elemental level. The total minimum of entropy number is constant regardless of the value of η. These results lead to another important design conclusion: for a given material and a fixed porosity, the minimum of entropy number does not depend on the characteristics of the collector.

7. Conclusion

This study showed that in the construction of tree-shaped architecture for gas and heat flow, the method of entropy generation minimisation is equivalent to minimizing driving forces in the case of single transfer phenomena. For coupled phenomena, this paper offers a new interesting alternative which consists of optimizing any coupled network. Kinetics has been neglected here, but it could be included in a more realistic solid–gas reactor model. Such a study would require numerical work, but the method continues to apply.

This study showed that for the improvement of exergy efficiency improvement it is important to focus on the design of an efficient heat and gas network architecture rather than enhancing the transport properties of the reactive material. All the optimised geometries have the same entropy generation number, since the heat of reaction r is fixed. Consequently, any specified material (conductivity, permeability, heat of reaction) will have its own optimum constructal network design, and, for a given solid–gas reaction, all these constructal reactors will have the same entropy generation.

In summary, the constructal method allowed us to develop the flow architecture for each available material. Because all the architecture have the same performance (heat and gas flow, entropy generation), the best design can be selected based on further economics or technical constraints.

Acknowledgements

The research reported in this paper is supported by a grant from the French Ministry of Education and Research.

References

[1] HPC'01, 2nd International Heat Powered Cycles conference, CDROM, ISBN 1-902038-01-0, Paris, 2001. Available from <http://hpc.01.free.fr>.
[2] B. Spinner, Changes in research and development of objectives for closed solid-sorption systems, keynote paper, in: Proceedings of International Absorption Conference, Montreal, 17–20 Sept, 1996.
[3] C. Coste, G. Crozat, S. Mauran, FR Patent No 8309885, 1983. Extension US Patent No. 4, 595, 774, 1986.
[4] R. Olives, S. Mauran, A highly conductive porous medium for solid–gas reactions: effect of the dispersed phase on the thermal tortuosity, Transport Porous Med. 43 (2001) 377–394.
[5] S. Mauran, L. Riguaud, O. Coudevylle, Application of the Carman–Kozeny correlation to a high-porosity and anisotropic consolited medium: The compressed expanded natural graphite, Transport Porous Med. 43 (2001) 355–376.
[6] P. Jolly, N. Mazet, Optimisation de la diffusion du gaz dans les matériaux réactifs, siège de transferts de chaleur, de masse et d'une réaction chimique, Int. J. Heat Mass Transfer 42 (1999) 303–321.
[7] N. Mazet, S. Mauran, P. Jolly, Dimensionless analysis of main limitation in solid–gas reactive blocks for solid sorption machines, in: Int. Sorption Heat Pump Conf., Munich, Germany, 1999.
[8] A. Bejan, Shape and Structure, from Engineering to Nature, Cambridge University Press, Cambridge, UK, 2000.
[9] A. Bejan, Constructal-theory network of conducting paths for cooling a heat generating volume, Int. J. Heat Mass Transfer 40 (4) (1997) 799–816.
[10] A. Bejan, Advanced Engineering Thermodynamics, second ed., Wiley, New York, 1997, Chapter 13.
[11] I. Prigogine, Introduction to Thermodynamics of Irreversible Processes, Wiley, New York, 1962.

[12] P. Neveu, Apports de la thermodynamique pour la conception et l'intégration des procédés, Research Habilitation Thesis (HDR), Université de Perpignan, December 2002.

[13] N. Mazet, H.-B. Lu, Improving the performance of the reactor under unfavourable operating conditions of low pressure, Appl. Thermal Eng. 18 (1998) 819–835.